Switched-Antenna Low-Frequency (LF) Radio-Frequency Identification (RFID) for Ornithology

Jon W. Wallace, *Senior Member, IEEE*, Leah C. Diamantides, *Student Member, IEEE*, Kwanho Claudia Ki, and Michael W. Butler

***Abstract*—Although low-frequency (LF) radio-frequency identification (RFID) is the de facto standard for many ornithological tracking studies, it is hampered by low range (5-10 cm) and the multiple tag collision problem. The simple concept of augmenting existing RFID transceivers with a switched antenna array is explored to overcome these difficulties. Analysis shows that non-ideal behavior of the switch elements can lead to detuning and cross-talk effects that should be considered when designing the LF antennas. An open-source prototype RFID reader with an integrated switch array supporting up to 12 antennas is developed and presented. Controlled laboratory tests indicate good read reliability of an 8-element antenna matrix covering a 37 cm × 37 cm ground area and a 4-element array placed on a bird feeder, but relative tag-antenna orientation must be carefully considered. A four-hour field test with tagged house sparrows indicates detection reliability of 94% and 78% for the 4-element feeder and 8-element mat arrays, respectively.**

***Index Terms*—Radiofrequency identification, antenna arrays, switches, animals, ornithology.**

I. Introduction

ANIMAL tracking has benefited immensely from developments in radio-frequency identification (RFID) technology over the last few decades [1], with applications ranging from livestock tracking [2]–[4] and pet identification [5] to managing endangered species [6]. RFID provides the ability to automatically identify, log the presence of, and even interact with individual animals, enabling new research in aquatic biology [7] game and wildlife [8], and insect studies [9], [10]. Our current interest in this technology is in the area of ornithology, where RFID opens many new lines of investigation [11].

RFID sensing of small bird species is challenging due to the tight size and weight requirements of tags coupled with the birds' high mobility. Passive low-frequency (LF) RFID operating in the 124-135 kHz range represents a mature technology that is attractive due to the small tag form factor, low cost, and insensitivity to wet media [12]. Two significant drawbacks of LF tags are the limited read range (5-10 cm) and the inability to simultaneously detect multiple tags (the collision problem). High-frequency (HF) tags operating at 13.56 MHz provide higher communications bandwidth, allowing faster detection and anti-collision protocols to be implemented. Unfortunately, HF tags are still a near-field technology, providing typical read range of 10 cm or less.

Given limitations of LF and HF technology, ultra-high frequency (UHF) RFID is expected to be the way forward for many applications. Commercial UHF tags operate in the 900 MHz band, allowing very fast scanning of multiple tags and providing read ranges of 10 m or more. Current UHF-RFID is a far-field technology, which requires tag size to be an appreciable fraction of the illumination wavelength (33 cm at 900 MHz). A sampling of recent research on "compact" UHF tags reveals tag areas ranging from 16 cm^2 to 34 cm^2 with corresponding read ranges from 9 m to 20 m [13]–[17]. UHF tags as small as 6 cm^2 are reported for "metal-mounted" tags, where a tagged metal object effectively becomes part of the tag's antenna [18]–[20].

Developments in UHF-RFID are exciting from an animal tracking perspective, but the small bird species in our studies have a cross-sectional area of 20 cm^2 or less, making existing UHF tags much too large for our purposes. As a comparison, small glass ampoule LF-RFID tags have a cross-sectional area of only 0.24 cm^2. Another concern is the robustness of UHF tags in the presence of wet biological or environmental media. The study in [21] indicates that UHF tag performance is severely degraded near water, even for near-field UHF tags. Although we expect limitations on UHF tag size and media sensitivity to eventually be solved, LF tags are currently the only viable option for studies on small bird species. Therefore, developing methodologies that can overcome range and collision limitations of LF tags is still of high interest.

The recent study in [22] considers LF tracking of bats over relatively large areas, which faces many of the same challenges as LF tracking of birds. The solution in [22] is a serialized coil architecture that allows the RFID antenna to occupy a large space, yet still maintain sufficient mutual inductance with tags for good read reliability. A similar concept is developed in [23] using antennas with multiple loops. However, the antennas in

Manuscript received November 13, 2019; revised January 16, 2020; accepted January 31, 2020. Date of publication February 4, 2020; date of current version May 25, 2020. This work was supported in part by the National Science Foundation Major Research Instrumentation (MRI) Program under Grant 1725970. *(Corresponding author: Jon W. Wallace.)*

Jon W. Wallace and Leah C. Diamantides are with the Department of Electrical and Computer Engineering, Lafayette College, Easton, PA 18042 USA (e-mail: wall@ieee.org; diamantl@lafayette.edu).

Kwanho Claudia Ki is with the Department of Biology, Utah State University, Logan, UT 84322 USA (e-mail: claudia.ki@usu.edu).

Michael W. Butler is with the Department of Biology, Lafayette College, Easton, PA 18042 USA (e-mail: butlermw@lafayette.edu).

Digital Object Identifier 10.1109/JRFID.2020.2971534

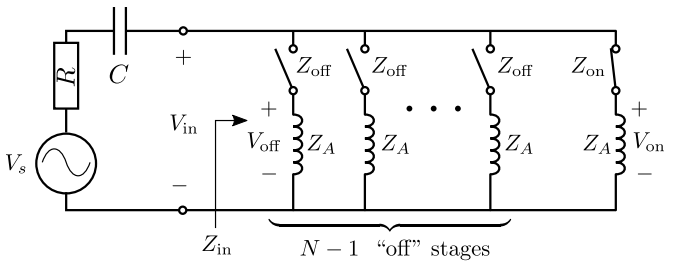

Fig. 1. Circuit model of the RFID switch array and driving circuit.

these studies are fairly complex, and these systems still exhibit the tag collision problem.

Although straightforward methods exist for identifying multiple RFID tags [24], [25], such anti-collision protocols are not implemented in commercial LF tags. In [26], multiple LF tags are identified and localized in a shelf structure, but tags had to be programmed with a set of special orthogonal codes. An alternative method was presented in [27] that identifies multiple LF tags using joint simultaneous detection with a software-defined radio. This approach avoids the need for specially programmed tags, but the required computational power may be prohibitive for low-cost, low-power sensor nodes.

Given the drawbacks of these methods, we explore a simpler approach in this paper, where a conventional RFID transceiver (similar to [28]) is connected to an array of loop antennas through low-cost switch elements. The system allows multiple tags to be identified over a wider area than the single-antenna system at the expense of longer scanning time. Tag localization was not a primary goal of our design, but we note that coarse localization is possible by recording which antenna is active when a tag is identified. More precise localization may be possible by extending the switched-array concept to large arrays with multiple active channels, but this is beyond the scope of our present work.

Although the switched LF-RFID idea is straightforward, we demonstrate that successful implementation requires careful consideration of the non-ideal behavior of the switch elements to mitigate detuning and cross-talk effects. We study the performance of switched-antenna LF RFID by developing a prototype reader and switch array capable of scanning up to 12 antennas, where hardware and software details (schematics, layout, firmware, etc.) are open source and provided free-of-charge to interested readers. Tag read reliability with respect to tag position and orientation is measured in a controlled lab environment. Finally, field tests are presented, indicating high read reliability for tagged house sparrows.

II. Switched RFID Reader Model

The switched RFID reader architecture can be represented in the simple form in Fig. 1. The RFID transceiver is represented as a sinusoidal source $v_s(t) = v_0 \sin(\omega t)$ in series with an RLC resonant circuit. The resistance R sets the quality factor of the resonator, limiting the voltage present across the inductor and widening the bandwidth. The resonator capacitance C together with the inductive load Z_{in} sets the resonant frequency of the system. In a traditional system, a single antenna would be connected to the source and RC circuit, such that $Z_{\text{in}} \approx j\omega L_{\text{in}}$, where L_{in} is the antenna inductance. In this case, the resonant frequency is given as $\omega = \omega_0 = (L_{\text{in}}C)^{-1/2}$.

TABLE I
Nominal Parameters of Switched Antenna Array Components

Parameter	Description	Value
C_{off}	Switch output capacitance in "off" state	20 pF
R_{on}	Switch output resistance in "on" state	16 Ω
L_A	Antenna inductance	1.35 mH
R_A	Antenna resistance	20 Ω
ω_0	Target resonant frequency	$2\pi\times$ 125 kHz

In our case, we replace the single antenna with the parallel switch network shown. Each of N RFID antennas is connected in a time-multiplexed fashion to the source-RC transceiver circuit. The dwell time on each antenna must be long enough to create sufficient magnetic energy around the antenna to power an RFID tag and allow the tag to transmit its information back by modulating the magnetic field.

Since the switch elements are not ideal short circuits or open circuits in the "on" and "off" states, respectively, the switch network will lead to modified antenna input impedance, reduction in the signal to the "on" antenna (insertion loss), and signal leakage to the "off" antennas (imperfect isolation). Here we analyze these effects, leading to basic design principles for the RFID antennas.

Note that we have analyzed more complicated arrangements than the simple parallel switches in Fig. 1. We have considered two switches per branch, but the improvement in isolation performance was minimal. A matrix arrangement was also analyzed, but isolation was significantly worse. Therefore, subsequent analysis only treats the simple parallel arrangement.

A. Input Impedance

Each of the $N-1$ "off" branches in Fig. 1 consists of a switch with impedance Z_{off} in series with the antenna having impedance $Z_A = R_A + j\omega L_A$, where R_A and L_A are the resistance and inductance of the antenna coil, respectively. Similarly, the single "on" branch consists of a switch with impedance Z_{on} in series with antenna impedance Z_A. At LF, switch impedance is often well approximated with $Z_{\text{on}} = R_{\text{on}}$ and $Z_{\text{off}} = 1/(j\omega C_{\text{off}})$. Impedance looking into the array is

$$Z_{\text{in}} = (Z_{\text{on}} + Z_A) \mathbin{/\!/} \left(\frac{Z_{\text{off}} + Z_A}{N-1}\right), \tag{1}$$

where $Z_1 \mathbin{/\!/} Z_2$ denotes the impedance of two loads Z_1 and Z_2 in parallel, given by $Z_1 Z_2/(Z_1 + Z_2)$. Due to the non-ideal behavior of the switches, $Z_{\text{in}} \neq Z_A$, thus changing the resonant frequency and quality factor of the effective RLC network, which in turn may reduce system performance.

To illustrate the effect of the switch network, numerical component values typical of the Atmel U2270B transceiver and IXYS CPC1017N switch that are used in this work are listed in Table I. Note that although the CPC1017N data sheet indicates a typical "off" capacitance of 5 pF, we have measured the capacitance of a PCB-mounted switch to have a typical value of $C_{\text{off}} \approx 20$ pF.

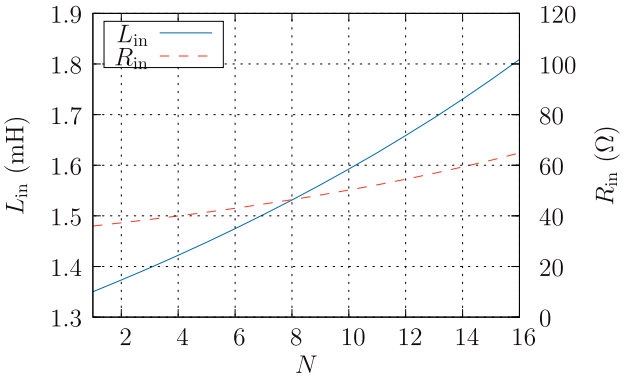

Fig. 2. Equivalent inductance and resistance seen looking into the switched array with N elements for the component values in Table I.

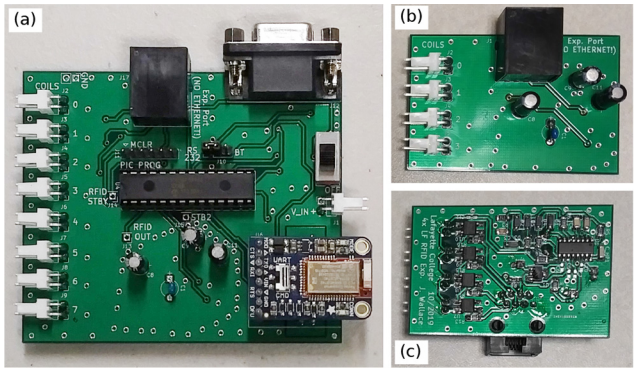

Fig. 3. Prototype RFID reader supporting up to 12 antennas: (a) main 8-antenna RFID reader board, (b) front and (c) back of the 4-antenna expansion module.

Fig. 2 plots input inductance and resistance of the switched antenna array with respect to the number of antennas (N). The input inductance increases rapidly with the number of antennas, which will detune the resonant frequency of the system. The effect can be compensated by designing antennas with lower inductance. For example, for $N = 8$, the choice of $L_A = 1.21$ mH results in $L_{\text{in}} = 1.35$ mH. An alternate option is to reduce the resonator capacitance, which for $N = 8$ would require a change from 1.2 nF to 1.06 nF to maintain a resonant frequency of 125 kHz.

B. Insertion Loss/Isolation

The insertion voltage loss ratio of the switch array can be quantified by computing the ratio

$$\text{IL} = \left|\frac{V_{\text{in}}}{V_{\text{on}}}\right| = \left|\frac{Z_A + Z_{\text{on}}}{Z_A}\right| = \left|\frac{R_A + j\omega L_A + R_{\text{on}}}{R_A + j\omega L_A}\right|. \quad (2)$$

The isolation voltage ratio can similarly be computed as

$$\text{ISO} = \left|\frac{V_{\text{on}}}{V_{\text{off}}}\right| = \left|\frac{Z_A + Z_{\text{off}}}{Z_A + Z_{\text{on}}}\right|. \quad (3)$$

These quantities can be expressed in dB using $\{\text{IL}, \text{ISO}\}_{\text{dB}} = 20\log_{10}\{\text{IL}, \text{ISO}\}$. Although these quantities are independent of N, increasing the number of antennas can decrease V_{in} if the resonator is not re-tuned, possibly leading to performance degradation. Using values from Table I and assuming re-tuning (V_{in} fixed), IL = 0.0035 dB and ISO = 35 dB, indicating that low loss and good isolation should be expected.

III. Prototype System

This section describes the salient features of the system design that are required to explore the switched-antenna RFID concept. For a more detailed description of the system, as well as free access to schematics, layout, firmware, etc., the interested reader is referred to [29].

A. RFID Reader

Our switched prototype RFID reader was largely inspired by the work in [28] and employs the Atmel U2270B RFID transceiver and PIC16F19156 microcontroller. The reader was designed in KiCAD and manufactured by PCBWay, as depicted in Fig. 3. The IXYS CPC1017N switch element was selected due to its low capacitance in the "off" state, as well as its ability to handle the high voltages ($\approx 50\ V_{\text{peak}}$) seen across LF RFID antennas at resonance. The reader employs eight switch elements to support an 8-element antenna array. An optional external module has an additional U2270B and four more switches, allowing a total of 12 antennas to be monitored. An Adafruit Bluetooth low-energy (BLE) module and Android app support wireless data download.

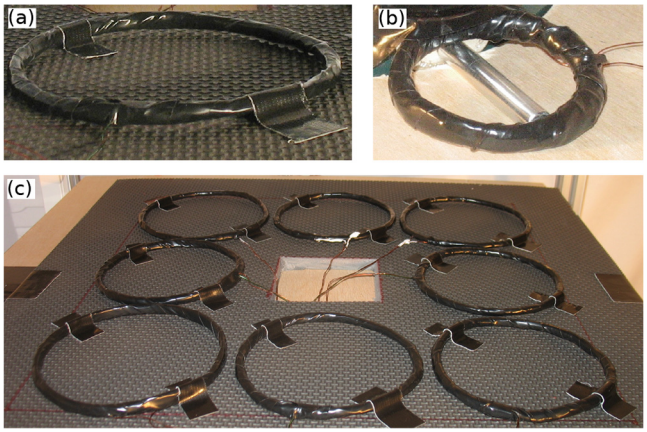

Fig. 4. RFID antennas used in this study: Single (a) 10-cm and (b) 4-cm loop antennas, and (c) 10-cm antennas mounted in a matrix on a foam mat.

B. Antenna Types

Two types of antennas have been used with the switched RFID reader, as depicted in Fig. 4. For covering large areas on the ground where birds are likely to forage, 10-cm diameter RFID antennas were constructed as shown in Fig. 4(a). To monitor areas near the perches on a feeder, smaller 4-cm diameter RFID antennas were constructed as shown in Fig. 4(b). The 10-cm antennas are attached to a foam mat, allowing a 37 cm × 37 cm area to be monitored as shown in Fig. 4(c).

Given the previous analysis of the switch array input impedance in Section II-A, we find that a lower antenna inductance of 1.21 mH should be used for the 8-element array of 10-cm antennas to achieve an array input inductance of 1.35 mH. The detuning effect on the 4-element array of 4-cm antennas is small, and therefore these antennas were simply

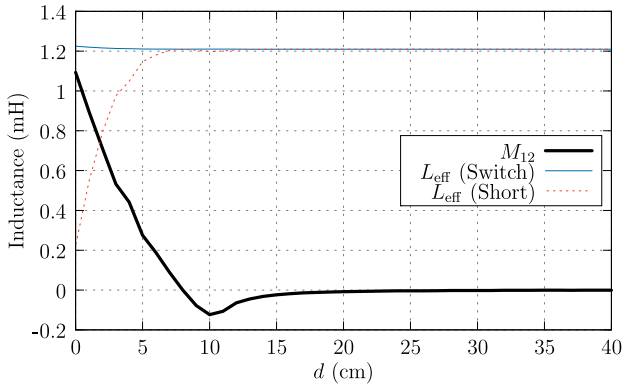

Fig. 5. The effect of mutual coupling for two 10-cm loop antennas placed beside each other with center-to-center spacing d, where M_{12} is the measured mutual impedance of the two loops, and L_{eff} (Switch) and L_{eff} (Short) denote the effective inductance of a driven antenna when the nearby coupled antenna is terminated with the switch "off" impedance and a short circuit, respectively.

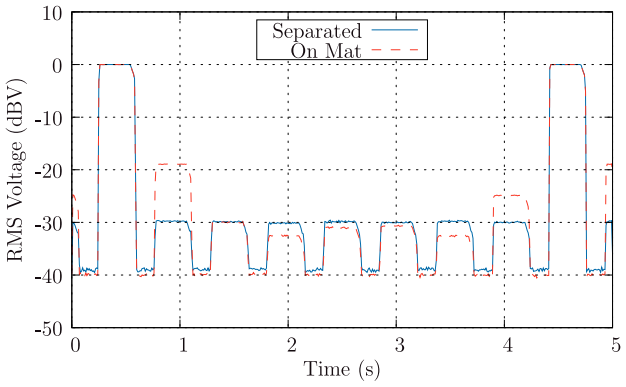

Fig. 6. Coupling measurement, which indicates the switch port isolation. The voltage across antenna $i = 1$ is probed while the RFID reader sequentially scans the 8-element array. RMS voltages have been smoothed and normalized to the voltage seen when antenna i is also the driven element.

designed to have an inductance of 1.35 mH, allowing them to also be used effectively with RFID readers not having the switch network.

An important consideration of the antennas in the matrix arrangement on the mat in Fig. 4(c) is mutual coupling of nearby elements, which can alter the input impedance of a driven element. To quantify this effect, we used a vector network analyzer at 125 kHz to measure the mutual inductance of two 10-cm loop antennas with a center-to-center spacing of d. Fig. 5 plots the mutual inductance M_{12}, showing that M_{12} is high (comparable to the self inductance of 1.21 mH) when antennas are directly on top of each other ($d = 0$), but quite low for side-by-side antennas ($d > 10$ cm). Two-port network theory can be used to quantify the effect that the nearby coupled antenna (Port 2) has on a driven antenna (Port 1). We have

$$Z_{\text{in},1} = Z_{11} - Z_{12}(Z_L + Z_{22})^{-1}Z_{21}, \tag{4}$$

where $Z_{\text{in},1}$ is the impedance looking into the driven element, $Z_{12} = Z_{21} = j\omega M_{12}$ is the mutual impedance, $Z_{11} = Z_{22} = R_A + j\omega L_A$ is the self antenna impedance, and Z_L is the load impedance on the coupled antenna. The effective inductance of the driven element is then $L_{\text{eff}} = \{Z_{\text{in}}\}/\omega$, where $\{\cdot\}$ takes the imaginary part. In our system, a non-driven element is connected to a switch in the "off" state, which presents impedance $Z_L = Z_{\text{off}}$. The effective impedance for this case is plotted in Fig. 5, as "L_{eff} (Switch)", showing that the deviation from the self-impedance is small in all cases, even for $d = 0$. We can consider a more extreme case where the coupled antenna is short-circuited, which would be appropriate in a system having multiple driven elements, and is plotted as "L_{eff} (Short)." In this case, having overlapping antennas severely affects L_{eff}, but interestingly, for $d > 10$ cm, the effect is still small. Since we only have a single driven element at a time and $d >= 12$ cm in our array, mutual coupling has a negligible impact on antenna impedance.

C. Isolation Measurement

Isolation was measured for the 8-element switched array by connecting eight 10-cm antennas to the eight ports of the switch and probing the voltage across the ith antenna coil. Measurements were performed with the antennas placed far apart (≈ 30 cm) to avoid RF coupling, and in the grid arrangement on the mat. Fig. 6 shows the smoothed RMS amplitude versus time for $i = 1$. Sampling this voltage at the middle of the kth burst is denoted V_{ik}, which is the voltage present on antenna i when antenna k is driven. The isolation between antennas k and i can then be estimated as $\text{ISO}_{ik} = V_{ii}/V_{ik}$.

For the case of separated antennas, port-to-port isolation is approximately 30 dB for all ports, somewhat worse than the 35 dB given by the idealized analysis previously. In the case of placement in the matrix on the mat, worst-case isolation is reduced to 19 dB for adjacent antennas due to RF coupling.

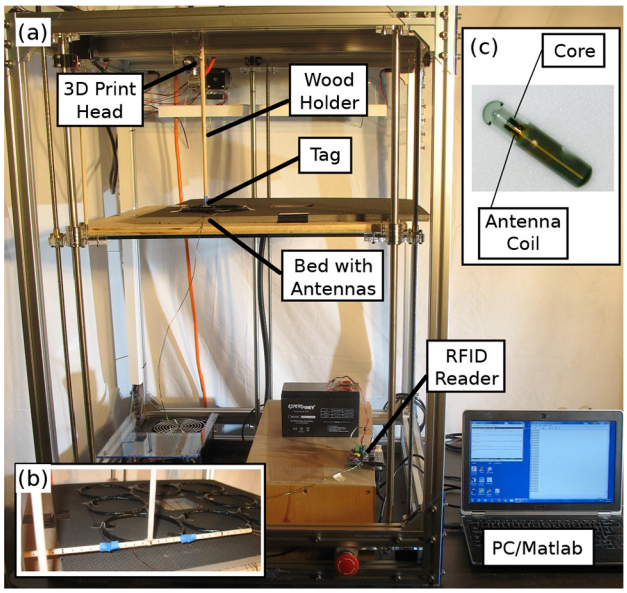

Fig. 7. System used to test the switched-antenna RFID prototype. (a) 3D-printer-based system showing a straight wooden holder for measuring single-tag read performance. (b) Wooden "tee" used to measure read performance with two tags. (c) Closeup of the type of LF-RFID tag used in this work.

IV. System Read Reliability Study

Fig. 7(a) shows a photo of the system used to test the read reliability of the switched-antenna RFID prototype. In this

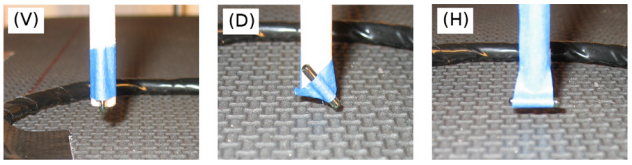

Fig. 8. RFID tag orientations used in measuring read performance: (V) vertical, (D) diagonal, and (H) horizontal.

setup, the antenna array is placed on the bed area of a three-dimensional (3D) printer, where the actual bed is replaced with a plywood board to avoid the presence of metal. RFID tags are placed on the end of a wooden holder connected to the 3D print head, allowing the tag to be moved to prescribed positions in a volume above the antennas. A PC running MATLAB sends serial commands to the 3D printer to move the head to precise locations on a specified 3D grid. For each sample point, the laptop queries the RFID reader over another serial interface to scan the antenna array M times. The number of successful tag identifications for each probed position is stored for further analysis. In all lab tests, each antenna was scanned with a 150-ms "on" time and 50-ms "off" time.

Two types of wooden holders are employed. For single-tag measurements, the straight probe in Fig. 7(a) is used, where the tag is taped at the bottom end of the holder. To test reading two tags tags in close proximity, the wooden "tee" holder in Fig. 7(b) is used instead of the straight bar, where two tags are taped to the bottom bar at a prescribed horizontal spacing. The LF RFID tags used in this test and employed in our field studies are 2×12 mm glass ampoule tags (EM4102 chip) from CYNTAG, Inc., a closeup of which is shown in Fig. 7(c). Fig. 8 shows the three different tag orientations that were considered in the measurements, which were accomplished by holding the tag with paper tape to the wooden holder at specific angles.

A. Single Antenna, Single Vertical Tag

As a baseline for read reliability, a single 10-cm antenna was attached to Port 1 of the prototype reader with the other ports left open. A single vertically oriented RFID tag was moved over an xy grid above the antenna plane using the 3D positioner. The vertical tag orientation is expected to be ideal, which can be understood by careful inspection of Fig. 7(c) showing a magnified view of the RFID tag. The tag contains a cylindrical ferrite core that runs along the axis of the tag, which is wrapped with fine copper wire forming the antenna coil. When the tag is vertical, the magnetic moment of the read coil on the mat is aligned with that of the antenna inside of the tag, and this will maximize coupling of the two coils. Fig. 9 plots the number of successful reads out of five scans at each position for 1-cm and 5-cm heights, indicating excellent read reliability within and slightly outside the read antenna coils.

B. 8-Element Array, Single Tag

The matrix arrangement of RFID antennas on the mat is likely to present the most difficulty in read reliability, due to coupling of the RFID antennas and interference of multiple RFID tags. Therefore, the performance of this arrangement

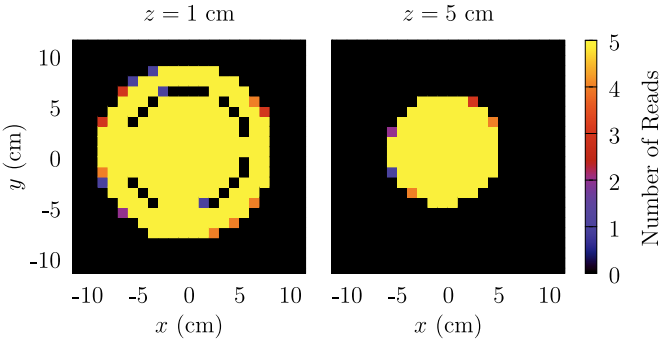

Fig. 9. Successful reads out of five scans for a vertically oriented RFID tag moved over a single 10-cm antenna.

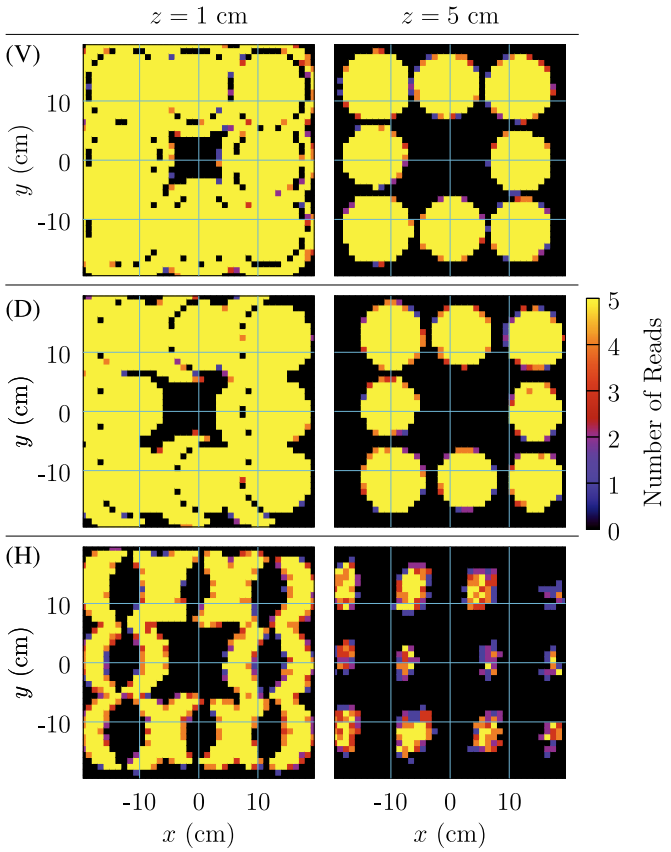

Fig. 10. Successful reads out of five scans for tags with vertical (V), diagonal (D), and horizontal (H) orientation moved over the 8-antenna element array of 10 cm antennas placed on a mat. Left and right columns of plots refer to read heights of 1 and 5 cm, respectively.

with respect to tag orientation and multiple tag separation has been carefully measured. The three different tag orientations that were considered are depicted in Fig. 8.

Fig. 10 presents the read reliability measured with the tag placed at 1-cm and 5-cm heights above the array for three orientations of the RFID tags. Vertical (V) orientation of the tag is expected to be optimal, since tag and reader coils are parallel. Horizontal (H) orientation is likely to give the poorest performance. For diagonal (D) orientation, the tag is placed at a 45° angle, half way between the V and H cases.

The results demonstrate that for a single tag that is vertically oriented, full detection is obtained nearly over the

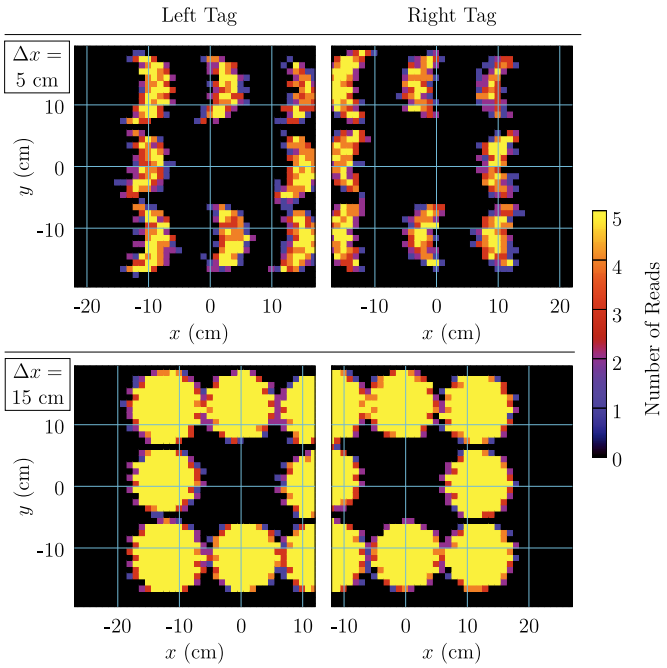

Fig. 11. Successful reads out of five scans for dual tags placed on the tee holder with either 5 cm or 15 cm inter-tag separation. The center of the T is scanned in a grid over the mat, and the x-axes have been shifted to correspond with the position of the tags. Read height was 5 cm.

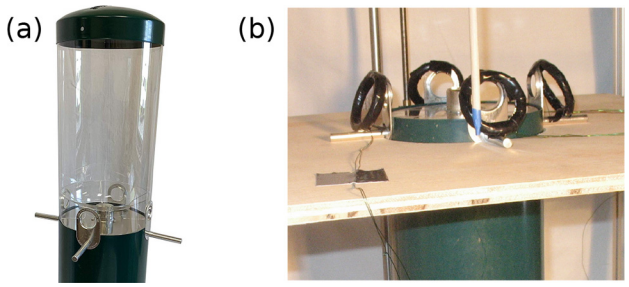

Fig. 12. (a) 4-position feeder used in Lafayette College ornithology studies. (b) Mounting of the reconfigured feeder in the 3D printer for testing.

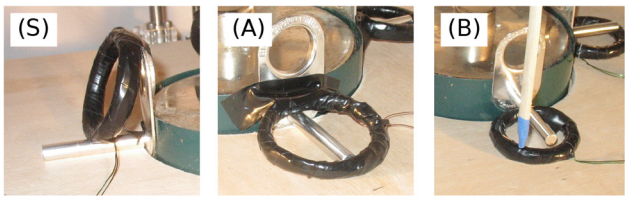

Fig. 13. Three different antenna orientations considered for feeder read reliability measurements: (S) slanted, (A) above perch, and (B) below perch.

complete mat at a low height (1 cm), and within 10 cm diameter discs above each antenna at the 5 cm height. Comparing with the single-antenna result in Fig. 9, this suggests that read performance is not significantly degraded due to impairments caused by the switch that were discussed in Section II. The results also indicate that sub-optimal tag orientation can degrade read reliability significantly. Since tags are attached parallel to birds' legs, and birds have bent legs when foraging on the ground, the diagonal arrangement is expected to be the typical case. As shown, the diagonal tag only suffers from a modest reduction in read reliability relative to the vertical case.

C. 8-Element Array, Dual Tags

One of the goals of the switched RFID concept was to allow multiple RFID tags to be identified in the same area with a single reader. One concern, however, is that tags may still interfere with each other if multiple tags are energized by the same antenna. To check read reliability with multiple tags, the tee holder in Fig. 7(b) was used with a horizontal distance of Δx between the tags. For each position, five scans of the array were initiated and the number of successful reads for each tag were stored.

Fig 11 shows dual tag read results for a read height of $z = 5$ cm with $\Delta x = 5$ cm and 15 cm. The left and right columns of plots correspond to identification of the left and right tags on the holder, respectively. For Δx =5 cm, it frequently happens that two tags are inside the lateral boundary of the same antenna. In this case, the signals from the two tags strongly interfere, and tag data is corrupted. However, for $\Delta x = 15$ cm, it is not possible for two tags to be within the boundary of the same antenna, and results look similar to the single-tag case. Note that for $\Delta x = 10$ cm (not plotted), results look very similar to $\Delta x = 15$ cm. For our application, these dual-tag results are encouraging, since it is expected that birds will be at least 10 cm apart.

D. 4-Element Array, Single Tag

Our target application requires identification of multiple birds simultaneously present at a feeder. The feeder used in current ornithology studies at Lafayette College is depicted in Fig. 12(a). One concern about this feeder is that it is constructed of metal, which might interfere with RFID antennas mounted on it. Also, it was unclear what orientation of antennas should be used to maximize identification of tags.

Fig. 12(b) shows how the feeder was probed using the 3D printer arrangement. The top part of the feeder (which is plastic) was removed to allow the RFID tag probe to reach the perch areas of the feeder. It is expected that the metal lid is far enough from the perches to be ignored, and therefore it was not used in measurements. A large hole was cut in a plywood board, allowing the perches to be placed at a convenient height for probing. The smaller 4-cm diameter RFID antennas were then placed near the four different perches and connected to four ports of the RFID reader. Three different orientations of the antennas were considered, as depicted in Fig. 13. First, antennas were placed at a slant from the feeder body to the perch, referred to as the slant (S) case. Second, antennas were placed above the perches and parallel to the ground, referred to as the above (A) case. Third, antennas were placed under the perches, also parallel to the ground, referred to as the below (B) case.

Read reliability was tested by scanning in a 3D volume above each perch, and the results are depicted in Fig. 14 for z heights of 1 cm and 3 cm. Although convenient for mechanical stability, the slanted arrangement (S) not only inhibits access to the feeder openings, but also the read range is suboptimal.

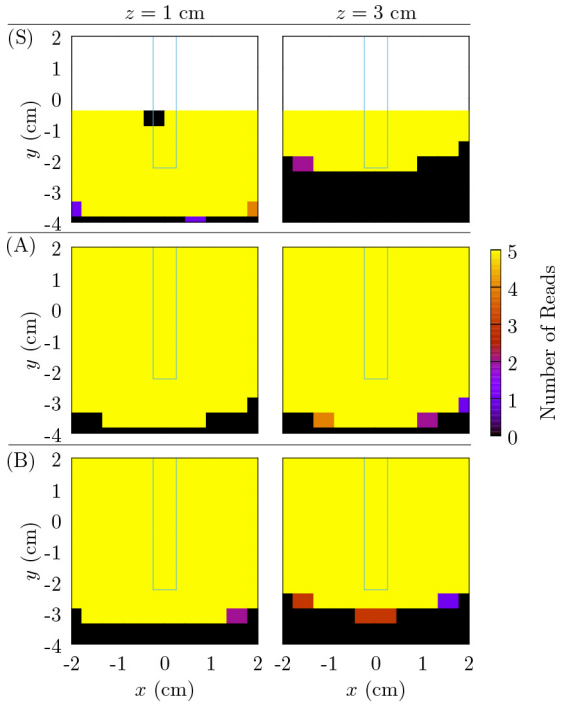

Fig. 14. Successful reads out of five scans for a single vertical tag moved in a 3D grid above the feeder perch. The 4-cm RFID antenna mounted on the perch was in one of three configurations in Fig. 13. Left and right columns of plots indicate tag heights of 1 cm and 3 cm above the perch. White space in the plots for (S) is area that could not be scanned due to the presence of the antenna. The cyan line indicates the extent of the aluminum perch.

Placing the RFID antenna immediately above the perch (A) provides the best read performance, but this location is also not convenient for birds landing on the perch. Since placing the antenna just below the perch (B) only slightly reduces read reliability, we will use this more convenient mounting location in subsequent field tests. It may be surprising that the presence of the metal perch in close proximity to the antenna has little effect on read reliability. However, the perch is a straight piece of metal (not a loop) and is made from non-ferrous metal (aluminum).

V. Field Test

To test identification reliability of RFID tags carried by small birds, the prototype RFID reader was deployed at the Metzgar Field complex at Lafayette College on the feeder station shown in Fig. 15 from 11:30 AM to 3:30 PM on July 16, 2019. The station consists of the 8-element array of 10-cm antennas in a matrix on a mat and the 4-element array of 4-cm antennas on the feeder. The RFID reader board and expansion module are placed in water-tight containers on the platform and on the feeder, respectively. System power is provided by a 12-V 8-Ah sealed lead acid battery, kept charged by a 5-W solar panel. The low-power nature of the system is well suited for field studies, requiring less than 0.5 W of power and running continuously without the need to replace batteries. A total of 121 house sparrows were tagged (see Fig. 16) in the spring and summer of 2019 prior to the test.[1]

[1]All work with animals was approved by Lafayette College's Institutional Animal Care and Use Committee, approval number 11042019M.

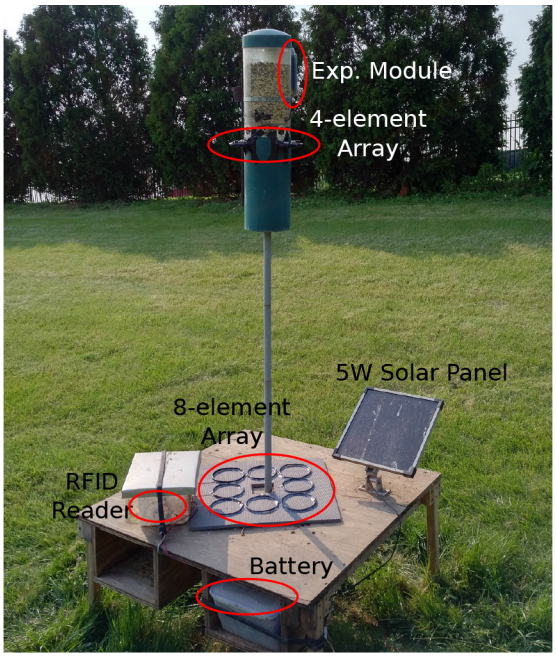

Fig. 15. Feeder station used in field tests and subsequent data collection.

Fig. 16. RFID tagging arrangement of house sparrows studied in this work. A glass LF RFID tag is enclosed in heat-shrink tubing (the black cylinder) and attached to colored bands that encircle the leg of the house sparrow.

Three video cameras were pointed at the station during the test, and subsequent comparisons of video footage with the RFID data log allowed detection rates to be assessed. Note that synchronization of video and RFID data was accomplished by placing a known tag near each antenna at the beginning of the test. The RFID reader was set to dwell for 150 ms on each antenna with a 100 ms "off" period between antennas, thus requiring 3 s to scan all 12 antennas.

A human observer watched the videos and created a spreadsheet logging each time a tagged bird landed on the station for at least 3 s (the array scan time), referred to as a "visit." For each visit, the following data was logged: arrival and departure time (to second precision), location (mat or feeder), and

TABLE II
DETECTION RESULTS

	Feeder (only)	Mat (only)	Feeder & Mat	Total
Unique Tags	6	2	1	9
Visits	86	23	-	109
Detections	81	18	-	99
Det. Rate	94%	78%	-	91 %

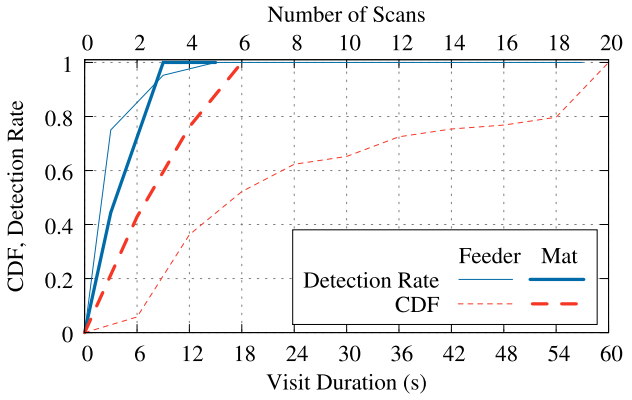

Fig. 17. Empirical cumulative distribution functions (CDFs) of visit duration and detection rate versus visit duration. For convenience, the top axis converts visit duration to the number of RFID scans obtained.

the feeder antenna index (for feeder visits). A MATLAB script was used to process the data. Visits that had at least one entry in the RFID log during the visit duration and at the the proper location were marked as "detected." Otherwise, visits were marked as "missed."

Table II summarizes the detection results. Although there were a significant number of visit events, only nine individuals (unique tags) were involved. Both the number of visits and the detection performance were better for the feeder compared to the mat. Interestingly, of the nine individuals who visited the station, six visited the feeder only, two visited the mat only, and only one visited both mat and feeder. This result suggests that even with lower detection performance, the mat may still be valuable for identifying individuals who avoid the feeder.

A more detailed picture of the detection statistics is provided in Fig. 17. Empirical cumulative distribution functions (CDFs) for feeder and mat visits were computed using a histogram with bin edges at $0, 2T, 4T, \ldots, 20T$, where T is the scan period of 3 s. Visits longer than $20T$ were lumped into the last bin. Average detection rates for visits in each bin were also computed and plotted at bin centers. Fig. 17 shows that visits to the feeder were typically much longer than those to the mat, which explains the poorer detection performance on the mat. For both the feeder and mat, detection rates increase steeply with the visit duration, where 100% detection was seen for visit lengths of 15 s (five scans) or longer.

For the few short visits that were missed detections, the video footage indicates some shortcomings of the system design. On the feeder, especially on short visits, birds may hold onto the RFID antenna with the tagged leg rather than grabbing the antenna holder or perch. This places the RFID tag axis almost parallel to the antenna, which is a poor read position/orientation. Aside from the problem of brief visits to the mat, it was noticed that birds spend most of the time on the wood area outside of the mat rather than standing on the mat itself. This suggests either using a larger mat with wider-spaced antennas or making the platform smaller.

VI. CONCLUSION

Although ornithological studies can benefit greatly from RFID technology, the size and weight constraints coupled with the high mobility of birds can hamper robust detection. Given that LF RFID tags are still the de facto standard for many animal-tracking studies, due to their small size and relative insensitivity to wet biological and environmental media, we explored the use of switched antenna arrays, covering larger scanning areas and overcoming the collision problem of multiple tags. Representing a natural extension of the architecture presented in [28], we have developed a prototype RFID reader that is low cost and low power, yet supports up to 12 antennas, allowing large feeding stations to be effectively monitored. The prototype reader is finding extensive use in ornithological studies at Lafayette College, which will appear in forthcoming publications. Given the open-source nature of the project, details of the hardware and software components are available online for interested researchers.

Tests conducted in this paper indicate encouraging detection rates for tagged birds, but also revealed possible areas of future improvement to the sensing concept. Identifying switch elements that have lower capacitance in the "off" state is highly desirable, since it would reduce the amount of antenna detuning, either allowing larger arrays to be employed or avoiding the need to change antenna inductance in modest-size arrays. Despite laboratory tests showing 100% detection reliability for the areas covered by RFID antennas, the field tests only exhibited about 90% reliability, due to unforeseen location and orientation of the tagged portion of birds' legs. In the future, it is expected that more optimal antenna structures and placement methods will be developed to allow near 100% detection reliability in the field.

We note that although the switched-array concept significantly extends the area of coverage for LF-RFID, read range from any given antenna is still around 10 cm. This range is sufficient for species that can be drawn to feeder perches or nearby foraging areas on the ground. We recognize, however, that these techniques are ineffective with many other bird species whose location cannot be easily controlled. We therefore anticipate developments in technologies providing longer inherent range, such as UHF-RFID, with high interest.

ACKNOWLEDGMENT

The authors thank Lafayette students D. A. Carroll for development of the RFID reader Bluetooth app, and E. N. Stierhoff and J. M. Carpenetti for help with the field test. They would also like to thank Eli Bridge for providing both RFID hardware as well as software support that were needed in the initial phase of this project.

REFERENCES

[1] R. E. Floyd, "RFID in animal-tracking applications," *IEEE Potentials*, vol. 34, no. 5, pp. 32–33, Sep./Oct. 2015.

[2] D. Talbot, "Where's the beef from?" *Technol. Rev.*, vol. 107, no. 5, pp. 48–56, Jun. 2004.
[3] B. Sechler, "Tech firms stampede to livestock," *Wall Street J.*, to be published.
[4] P. Barge, P. Gay, V. Merlino, and C. Tortia, "Radio frequency identification technologies for livestock management and meat supply chain traceability," *Can. J. Animal Sci.*, vol. 93, no. 1, pp. 23–33, Mar. 2013.
[5] A. Schwalm and H. Georg, "Electronic animal identification—ISO-standards and current situation in Germany," *Landbauforschung*, vol. 61, no. 4, pp. 283–288, Dec. 2011.
[6] P. O'Donoghue and C. Rutz, "Real-time anti-poaching tags could help prevent imminent species extinctions," *J. Appl. Ecol.*, vol. 53, no. 1, pp. 5–10, Jul. 2016.
[7] R. J. Lennox *et al.*, "Envisioning the future of aquatic animal tracking: Technology, science, and application," *BioScience*, vol. 67, pp. 884–896, Oct. 2017.
[8] J. M. Craine, E. G. Towne, and A. Elmore, "Intra-annual bison body mass trajectories in a tallgrass prairie," *Mammal Res.*, vol. 60, no. 3, pp. 263–270, Jul. 2015.
[9] P. de Souza *et al.*, "Low-cost electronic tagging system for bee monitoring," *Sensors*, vol. 18, no. 7, pp. 1–21, Jul. 2018.
[10] P. Nunes-Silva *et al.*, "Applications of RFID technology on the study of bees," *Insectes Sociaux*, vol. 66, no. 1, pp. 15–24, Feb. 2019.
[11] D. N. Bonter and E. S. Bridge, "Applications of radio frequency identification (RFID) in ornithological research: a review," *J. Field Ornithol.*, vol. 82, no. 1, pp. 1–10, Mar. 2011.
[12] V. Chawla and D. S. Ha, "An overview of passive RFID," *IEEE Commun. Mag.*, vol. 45, no. 9, pp. 11–17, Sep. 2007.
[13] Y.-H. Lee, E.-H. Lim, F.-L. Bong, and B.-K. Chung, "Bowtie-shaped folded patch antenna with split ring resonators for UHF RFID tag design," *IEEE Trans. Antennas Propag.*, vol. 67, no. 6, pp. 4212–4217, Jun. 2019.
[14] A. Choudhary, D. Sood, and C. C. Tripathi, "Wideband long range, radiation efficient compact UHF RFID tag," *IEEE Antennas Wireless Propag. Lett.*, vol. 17, no. 10, pp. 1755–1759, Oct. 2018.
[15] H. Li, J. Zhu, and Y. Yu, "Compact single-layer RFID tag antenna tolerant to background materials," *IEEE Access*, vol. 5, pp. 21070–21079, 2017.
[16] J.-H. Lu and B.-S. Chang, "Planar compact square-ring tag antenna with circular polarization for UHF RFID applications," *IEEE Trans. Antennas Propag.*, vol. 65, no. 2, pp. 432–441, Feb. 2017.
[17] H.-D. Chen, C.-Y.-D. Sim, C.-H. Tsai, and C. Kuo, "Compact circularly polarized meandered-loop antenna for UHF-band RFID tag," *IEEE Antennas Wireless Propag. Lett.*, vol. 15, pp. 1602–1605, 2016.
[18] W.-H. Ng, E.-H. Lim, F.-L. Bong, and B.-K. Chung, "Compact planar inverted-S antenna with embedded tuning arm for on-metal UHF RFID tag design," *IEEE Trans. Antennas Propag.*, vol. 67, no. 6, pp. 4247–4252, Jun. 2019.
[19] C.-W. Moh, E.-H. Lim, F.-L. Bong, and B.-K. Chung, "Miniature coplanar-fed folded patch for metal mountable UHF RFID tag," *IEEE Trans. Antennas Propag.*, vol. 66, no. 5, pp. 2245–2253, May 2018.
[20] A. Sharma, A. T. Hoang, F. Nekoogar, F. U. Dowla, and M. S. Reynolds, "An electrically small, 16.7 m range, ISO18000-6C UHF RFID tag for industrial radiation sources," *IEEE J. Radio Freq. Identification*, vol. 2, no. 2, pp. 49–54, Jun. 2018.
[21] S. R. Aroor and D. D. Deavours, "Evaluation of the state of passive UHF RFID: An experimental approach," *IEEE Syst. J.*, vol. 1, no. 2, pp. 168–176, Dec. 2007.
[22] A. Diet *et al.*, "Flexible serialized complementary coils for the detection of moving LF RFID tags," *IEEE J. Radio Freq. Identification*, vol. 3, no. 3, pp. 183–190, Sep. 2019.
[23] K. Wang *et al.*, "Detecting range and coupling coefficient tradeoff with a multiple loops reader antenna for small size RFID LF tags," in *Proc. IEEE Int. Conf. RFID Technol. Appl. (RFID-TA)*, Nov. 2012, pp. 154–159.
[24] Q. Zhihong and W. Xue, "An overview of anti-collision protocols for radio frequency identification devices," *China Commun.*, vol. 11, no. 11, pp. 44–59, Nov. 2014.
[25] A. A. Mbacke, N. Mitton, and H. Rivano, "A survey of RFID readers anticollision protocols," *IEEE J. Radio Freq. Identification*, vol. 2, no. 1, pp. 38–48, Mar. 2018.
[26] R. Psiuk *et al.*, "Simultaneous 2D localization of multiple standard passive LF-RFID transponders," in *Proc. IEEE Int. Conf. RFID Technol. Appl. (RFID-TA)*, Sep. 2018, pp. 1–6.
[27] D. Shen, G. Woo, D. P. Reed, A. B. Lippman, and J. Wang, "Separation of multiple passive RFID signals using software defined radio," in *Proc. IEEE Int. Conf. RFID*, Apr. 2009, pp. 139–146.
[28] E. S. Bridge and D. N. Bonter, "A low-cost radio frequency identification device for ornithological research," *J. Field Ornithol.*, vol. 82, no. 1, pp. 52–59, Mar. 2011.
[29] J. W. Wallace, *Lafayette College Switched LF RFID Reader*, Lafayette College, Easton, PA, USA, 2019. [Online]. Available: http://jonwallace.org/

Jon W. Wallace (Senior Member, IEEE) received the B.S. and Ph.D. degrees in electrical engineering from Brigham Young University, Provo, UT, USA, in 1997 and 2002, respectively. He was with Jacobs University, Bremen, Germany, from 2006 to 2013. Since 2014, he has been with the Department of Electrical and Computer Engineering, Lafayette College, Easton, PA, USA. His research interests include physical layer security, MIMO systems, unmanned aircraft systems, and applications of radio-frequency identification. He serves as an Associate Editor for the IEEE TRANSACTIONS ON AEROSPACE AND ELECTRONIC SYSTEMS.

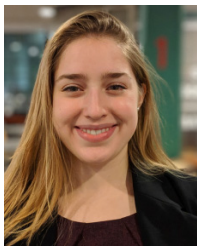

Leah C. Diamantides (Student Member, IEEE) is currently pursuing the B.S. degree in electrical and computer engineering with Lafayette College, Easton, PA, USA, where she conducted research in radio-frequency identification. Upon graduation, she will be working as a Firmware Engineer with Microsoft, Seattle, WA, USA. Her other interests include embedded systems and control systems.

Kwanho Claudia Ki received the B.S. degree in biology from Lafayette College, Easton, PA, USA, in 2019. She is currently pursuing the Ph.D. degree in biology with Utah State University, Logan, UT, USA. During her undergraduate education, she studied the physiology and behavior of passerine birds. Her current research interests include eco-immunology, conservation, and the reproductive and oxidative physiology of reptiles.

Michael W. Butler received the B.A. degree in biology and physics from Bowdoin College, Brunswick, ME, USA, in 2002, the M.S. degree in raptor biology from Boise State University, Boise, ID, USA, in 2006, and the Ph.D. degree in biology from Arizona State University, Tempe, AZ, USA, in 2012. Since 2012, he has been a Professor with the Department of Biology, Lafayette College, Easton, PA, USA. His current research interests include ecological immunology, oxidative physiology, behavioral ecology, and the evolutionary consequences of these processes.